
This is an electronic reprint of the original article.
This reprint may differ from the original in pagination and typographic detail.

Author(s): Majumdar, Sayani & Dey, Sukumar & Huhtinen, Hannu & Dahl, Johnny & Tuominen, Marjukka & Laukkanen, Pekka & van Dijken, Sebastiaan & Majumdar, Himadri S.

Title: Comparative study of spin injection and transport in Alq3 and Co phthalocyanine-based organic spin valves

Year: 2014

Version: Post print

Please cite the original version:

Majumdar, Sayani & Dey, Sukumar & Huhtinen & Hannu & Dahl, Johnny & Tuominen, Marjukka & Laukkanen, Pekka & van Dijken, Sebastiaan & Majumdar, Himadri S. 2014. Comparative study of spin injection and transport in Alq3 and Co phthalocyanine-based organic spin valves. Spin. Volume 04, Issue 02. 1440009. ISSN 2010-3247 (printed). DOI: 10.1142/s2010324714400098

Rights: © 2014 World Scientific Pub Co Pte Lt. Electronic version of an article Majumdar, Sayani & Dey, Sukumar & Huhtinen & Hannu & Dahl, Johnny & Tuominen, Marjukka & Laukkanen, Pekka & van Dijken, Sebastiaan & Majumdar, Himadri S. 2014. Comparative study of spin injection and transport in Alq3 and Co phthalocyanine-based organic spin valves, published as Spin, Volume 04, Issue 02. 1440009. ISSN 2010-3247 (printed). DOI: 10.1142/s2010324714400098. <http://www.worldscientific.com/>.

All material supplied via Aaltodoc is protected by copyright and other intellectual property rights, and duplication or sale of all or part of any of the repository collections is not permitted, except that material may be duplicated by you for your research use or educational purposes in electronic or print form. You must obtain permission for any other use. Electronic or print copies may not be offered, whether for sale or otherwise to anyone who is not an authorised user.

Comparative study of spin injection and transport in Alq₃ and Co-Phthalocyanine based organic spin valves

Sayani Majumdar^{1,2*}, Sukumar Dey^{3,4}, Hannu Huhtinen², Johnny Dahl⁵, Marjukka Tuominen⁵
Pekka Laukkanen⁵, Sebastiaan van Dijken¹ and Himadri S. Majumdar^{4,6}

¹ Nanospin, Department of Applied Physics, Aalto University School of Science, P.O. Box 15100, FI-00076 Aalto, Finland.

² Wihuri Physical Laboratory, Department of Physics and Astronomy, University of Turku, 20014 Turku, Finland.

³ Department of Solid State Physics, Indian Association for the Cultivation of Science, Jadavpur 700032, Calcutta, India.

⁴ Fysik, Åbo Akademi University, 20050 Turku, Finland.

⁵ Materials Research Laboratory, Department of Physics and Astronomy, University of Turku, 20014 Turku, Finland.

⁶ VTT Technical Research center of Finland, FI-02150 Espoo, Finland.

Abstract

Recent experimental reports suggest the formation of a highly spin-polarized interface (“spinterface”) between a ferromagnetic Co electrode and a metal-phthalocyanine molecule. Another report shows an almost 60% giant magnetoresistance (GMR) response measured on Co/H₂Pc-based single molecule spin valves. In this article, we compare the spin injection and transport properties of organic spin valves with two different organic spacers, namely Tris(8-hydroxyquinolato) aluminium (Alq₃) and Cobalt-Phthalocyanine (CoPc) sandwiched between half-metallic La_{0.7}Sr_{0.3}MnO₃ (LSMO) and Co electrodes. Alq₃-based spin valves exhibit clear and reproducible spin valve switching with almost 35% negative GMR at 10 K, in accordance with previous reports. In contrast, CoPc-based spin valves fail to show clear GMR response above noise level despite high expectations based on recent reports. Investigations of electronic,

* Corresponding author e-mail: sayani.majumdar@aalto.fi

magnetic and magnetotransport properties of electrode/spacer interfaces of LSMO/CoPc/Co devices offer three plausible explanations for the absence of GMR: (1) CoPc films are strongly chemisorbed on the LSMO surface. This improves the LSMO magnetic properties but also induces local traps at the LSMO interface for spin-polarized charge carriers. (2) At the Co/CoPc interface, diffusion of Co atoms into the organic semiconductor (OS) layer and chemical reactivity between Co and the OS deteriorates the ferromagnetic properties of Co. This renders the Co/CoPc interface as unsuitable for efficient spin injection. (3) The presence of heavy Co atoms in CoPc leads to large spin-orbit coupling in the spacer. The spin relaxation time in the CoPc layer is therefore considerably smaller compared to Alq₃. Based on these findings, we suggest that the absence of GMR in CoPc-based spin valves is caused by a combined effect of inefficient spin injection from ferromagnetic contacts and poor spin transport in the CoPc spacer layer.

1. Introduction

Spintronics is the emerging branch of condensed matter physics where in addition to the electronic charge, electron spins also carry information and spin quantum states are actively manipulated using external magnetic fields [1, 2]. Control over both the charge and spin of carriers enables multi-functionality, lower power consumption, increased integration density, and many other advantages to present day electronics. Organic or hybrid inorganic-organic spintronics is a new addition to this rapidly developing field where advantages of large spin polarization of ferromagnetic (FM) metals and half-metals and long spin decoherence times of organic semiconductors (OS) are explored [3–6].

Organic spintronics is one of the major developments in the field of spintronics. In the past decade, several groups extensively investigated the spin injection and transport properties of different small molecules and polymeric OSs [7–9]. While many studies show significant giant or tunneling magnetoresistance (GMR or TMR respectively) for FM/OS/FM vertical spin-valve structures [8–12] and magnetic tunnel junctions (MTJs) [13, 14], there are also reports on the complete absence of spin injection in OSs [15]. Recently, it was found that the Hanle effect, one of the major criteria for confirming spin injection in conventional semiconductors, is missing from OS-based spintronic devices [16]. However, it is not clear whether the Hanle effect can be expected in systems where spin transport mainly occurs via incoherent hopping. Hence, spin injection and transport in OSs remain a matter of intense scientific discussion and debate.

Another important issue is the temperature dependence of the spin decoherence length in OSs. Previously, it was shown that the spin decoherence length in OSs is more or less temperature independent [17] and the loss of GMR signal in organic spintronic devices is mainly due to a decrease of spin polarization in half-metallic LSMO electrodes. Recent spectroscopy [18] and transport results indicate that besides the loss of spin polarization in LSMO, the spin relaxation in organic materials also increases with increasing temperature [19, 20]. In addition, the FM/OS interface is another important factor for efficient device performance and, despite some interesting results [21–25], the interface interaction mechanisms are not fully understood.

Magnetic field effects in OSs and their influence on the spin polarization of carriers inside organic spin valves is another relevant issue. In conventional spin valves and MTJs, the spacer or barrier layer consists of non-magnetic metals or dielectrics and the carriers are not affected by the magnetic field when passing through these layers. However, this is not the case in

organic devices. OSs do not have a well-defined band structure where delocalization of charge carriers can take place. In OSs, strong carbon-carbon bonds and weak van der Waals interactions between molecules result in transport properties that are mainly determined by intermolecular interactions. In most OSs, charge transport takes place through hopping between pseudo-localized states. The motion of charge carriers via hopping can be significantly altered under the influence of an external magnetic field. Therefore, a sizable magnetoresistance effect, commonly known as organic magnetoresistance (OMAR), has been found in organic light emitting diodes [26], transistors [27] and single films without any FM electrodes. Although the exact origin of OMAR is still under debate, it is known that hyperfine fields inside the OS [28] and the presence of both types of carriers (electrons and holes) [29] contribute to large magnetic field effects. In hydrocarbons, for example, spin-polarized carriers precess around local hyperfine fields and this causes the carriers to lose their initial spin orientation. Therefore, it has been suggested that OSs with small hyperfine fields could be an ideal choice for obtaining large spin relaxation lengths and significant GMR responses in spin-valve devices with relatively thick barriers [28]. Also experimentally the role of hyperfine interaction has been demonstrated [30]. Due to the presence of shallow (~ 0.1 eV) and deep (~ 0.5 eV) trap states and impurities, the charge carrier mobility of OSs is several orders of magnitude smaller than that of inorganic semiconductors (high quality Si single crystals have a mobility of $\sim 10^3$ cm² V⁻¹s⁻¹). This often leads to a time-dependent OMAR effect where the magnitude of the magneto-resistance depends on the scan speed of the external magnetic fields. Large hysteretic OMAR responses have been observed in devices with different OSs [31, 32]. Therefore, to work as an efficient spin transporting layer, it is of the utmost importance to utilize an OS material with high charge carrier mobility.

Among different OSs, metal-phthalocyanines are widely studied for different electronic applications such as catalytic, opto-electronic and photovoltaic devices as these molecules exhibit robust thermal and chemical stability and tunable electronic and optical properties [33–36]. Selection of the central metal atom and side groups can dramatically influence the electronic and magnetic properties of the phthalocyanine compounds due to variation in the number of unpaired electrons. Also, depending on the electronic and magnetic properties, the degree and nature of interactions with FM electrodes change and this can have significant consequences for the spin injection properties of organic spin valves.

When a transition-metal atom (Fe, Co) is placed in the center of the phthalocyanine ring, the ground state configuration varies depending on the ligand field splitting, which causes a substantial variety of electronic and magnetic ground states. For instance, the magnetic properties of Cobalt-phthalocyanine with molecular formula $C_{32}H_{16}CoN_8$ (CoPc), arise from unpaired spins in the $3d$ orbitals of the central atom. CoPc has a magnetic moment of $1.09 \mu_B$ [37] (much smaller than the isolated Co^{2+} ion, i.e., $5\mu_B$), but as a free molecule it is paramagnetic. A recent experimental study suggests the formation of a highly spin-polarized interface (“spinterface”) between a ferromagnetic Co electrode and a Mn-phthalocyanine molecule [23], which is extremely promising for spintronics. Also, a GMR effect of almost 60% has been achieved with Co/ H_2Pc -based single molecule spin valves [38].

In the present work, we investigate the spin-injection and transport properties of half metallic oxide $La_{0.7}Sr_{0.3}MnO_3$ (LSMO) and CoPc-based spin valves with a Co top electrode (i.e. LSMO/CoPc/Co). The properties of this spin valve are compared with Tris(8-hydroxyquinolino) aluminium (Alq_3)-based spin valves prepared under the same conditions. Alq_3 is one of the most studied OS spacer materials for organic spin valves. LSMO, a well-known half metallic complex oxide, is used for its 100% spin-polarized conduction band and well-matched carrier density and workfunction with most OSs [39]. Devices fabricated under similar conditions show completely different spin injection and transport behavior and these differences are investigated and discussed in terms of the electronic and transport properties of the FM/CoPc interface and spin transport through the CoPc molecules.

2. Experimental

LSMO films with a thickness of 150 nm and a surface roughness of ~ 4 nm were grown on single crystalline $SrTiO_3$ (001) substrates using pulsed laser deposition (for details see Ref. 40). After removing the LSMO film from the PLD chamber, it was cleaned with acetone and isopropyl alcohol and mounted into a thermal evaporator. Either a 120 nm thick CoPc or Alq_3 layer was subsequently deposited on LSMO. A ferromagnetic layer of Co with a thickness of 8-10 nm was deposited on top of the OS films through a mask and it was capped by an Al layer to prevent oxidation of the Co. All vacuum depositions were conducted under a pressure of 5×10^{-6} mbar. The effective area of the devices was 2 mm \times 2 mm. After fabrication, the samples were transferred to a cryostat and current-voltage (I - V) characteristics were measured at 10 K, 50 K,

and 100 K. GMR at different bias voltages and temperatures were measured by sweeping the magnetic field between +300 mT and -300 mT. Magnetization measurements as a function of temperature ($M-T$) and magnetic field ($M-B$) were conducted using a SQUID magnetometer. Photoemission spectra were measured using a Perkin-Elmer PHI 5400 spectrometer with a monochromatized Al $K\alpha$ x-ray source that was operated at 14 keV. The analyzer pass energy was 18 eV.

3. Results and discussions

3.1. Magneto-transport properties of organic spin valves

a. LSMO/CoPc/Co/Al

The inset of Figure 1 shows a schematic diagram of the device structure. The $I-V$ curves of the spin valve devices at 10 K, 50 K, and 100 K (main panel of Figure 1) show a clear nonlinear behavior which increases strongly with decreasing temperature. This response indicates the formation of a Schottky barrier at the FM/OS interface and it confirms the absence of metal shorts through the organic spacer. An asymmetry in the $I-V$ characteristics is observed. This is attributed to a difference in the injection barriers of the LSMO and Co electrodes with the highest occupied molecular orbital (HOMO) and lowest unoccupied molecular orbital (LUMO) level of CoPc molecules. From the $I-V$ characteristics, it can be clearly seen that the injection barrier is higher for negative bias voltages. Since negative bias represents carrier transport from the Co to the LSMO side, it can be inferred that the injection barrier height is greater on the Co side. Based on the unperturbed band diagram (left panel of Fig. 1), the work function of the LSMO and Co electrodes are very similar and therefore this should not result in an asymmetric $I-V$ curve. The observed asymmetry thus indicates a significant change of the interface energetics by interactions between the CoPc molecules and the FM electrodes. Such changes can occur either through interface dipole formation or chemical reactions, which both result in a modification of the injection barriers.

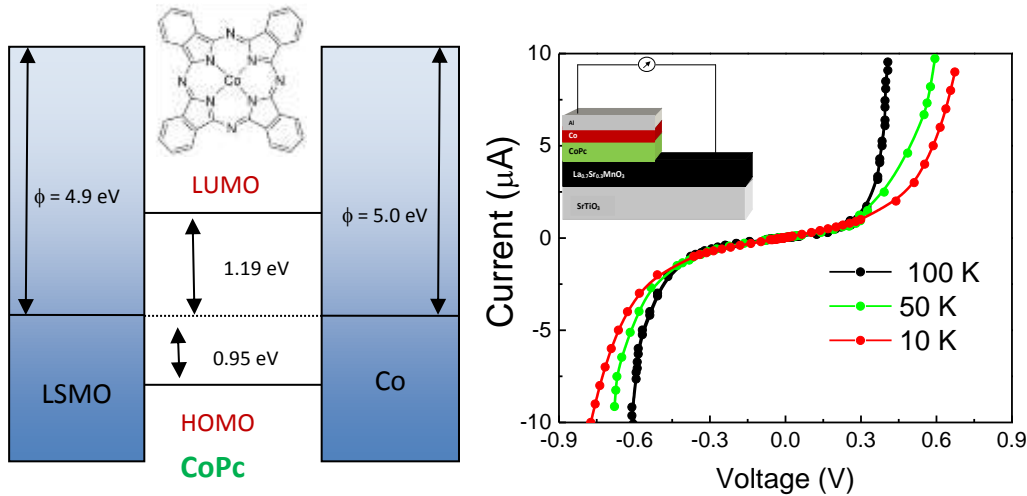


Fig. 1. Chemical structure of the CoPc molecule and energy band diagram of the spin valve device (left panel) and I - V curves of a LSMO/CoPc/Co/Al spin valve measured at different temperatures (right panel). The inset of the right panel shows a schematic diagram of the device.

Despite the good I - V characteristics, magnetotransport measurements at different device currents do not show any significant GMR response (Figure 2), even at 10 K where the LSMO electrode exhibits almost 100% spin polarization. The noise level in the measurements is about 3% for bias currents of 1 μA and 1.5 μA and it is slightly larger for a current of 2 μA . From this we conclude that the GMR response is well below 3%, if any at all, in CoPc-based spin-valve devices. The absence of a clear GMR signal indicates inefficient spin injection or detection, small spin-life time inside the CoPc spacer layer, or a combination of both effects.

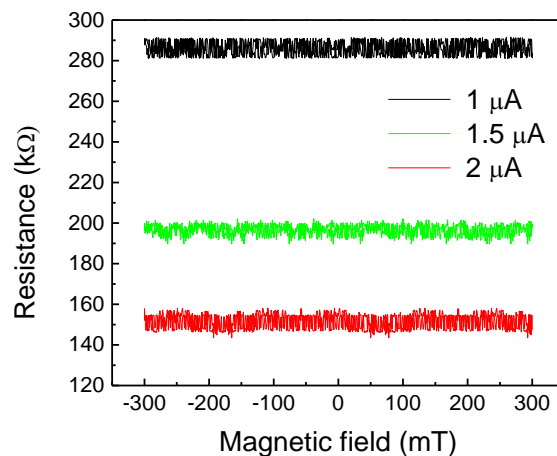


Fig. 2. LSMO/CoPc/Co device resistance measured as a function of in-plane external magnetic field at three different device currents at 10 K.

b. LSMO/Alq₃/Co/Al

Spin-valve devices with Alq₃ spacers also show nonlinear *I-V* characteristics at 10 K, 50 K, and 100 K (Figure 3). Although a little asymmetry in the *I-V* curves is present, it is considerably smaller compared to CoPc-based devices. Thus, the injection barrier heights from the LSMO and Co sides are nearly identical in the Alq₃-based devices, as expected from their unperturbed band diagram (left panel of Figure 3). From this we conclude that the interface reaction between organic molecules and FM electrodes is not the same for all OS materials. This is especially true for Co which tends to penetrate into soft organic layers and form nano-islands.

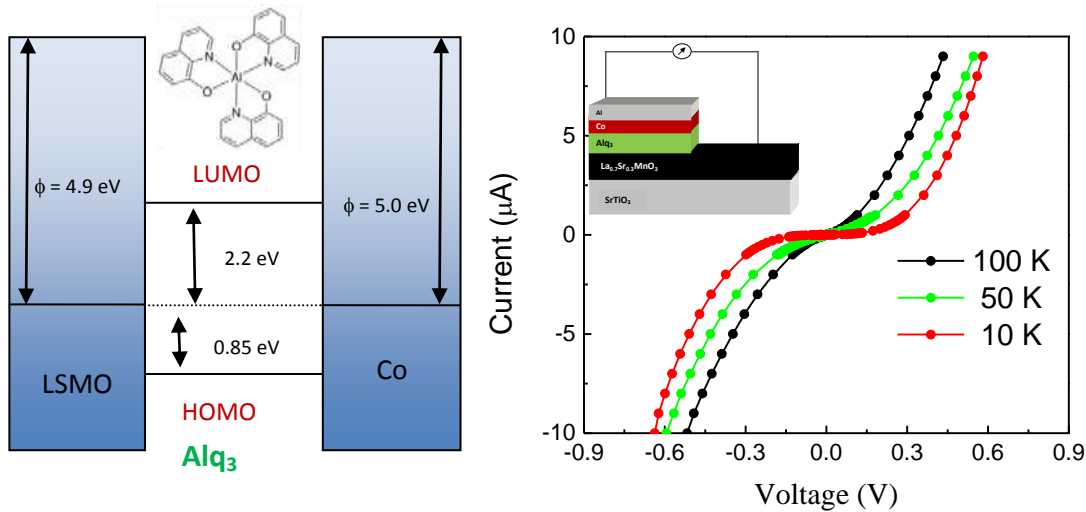


Fig. 3. Chemical structure of the Alq₃ molecule and energy band diagram of the spin-valve device (left panel) and *I-V* characteristic of a LSMO/Alq₃ (120 nm)/Co (8 nm)/Al (100 nm) spin valve at different temperatures (right panel). The inset of the right panel shows a schematic diagram of the device.

Magnetotransport measurements on spin valves with an Alq₃ spacer show a clear and reproducible GMR response. Figure 4 compares the GMR effect at different temperatures. Here, GMR is defined as $GMR = (R_{AP} - R_P) / R_{AP}$, where R_P and R_{AP} are the device resistances for parallel (*P*) and anti-parallel (*AP*) magnetization alignment, respectively. At 10 K, a large negative GMR of almost 30% is observed for a current of 1 μA and the magnetic moments of the LSMO and Co electrodes switch abruptly. The GMR response decreases with increasing temperature.

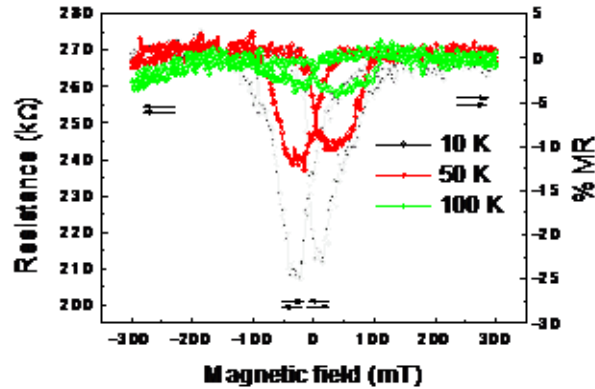


Fig. 4. Resistance of a LSMO/Alq₃/Co organic spin valve as a function of in-plane magnetic field obtained at three different temperatures and a constant current of 1 μ A.

Figure 5 shows the GMR response at 10 K for device currents of 1 μ A, 1.5 μ A and 2 μ A. Clearly, the GMR effect decreases and switching between *P* and *AP* magnetization states becomes more gradual with increasing current.

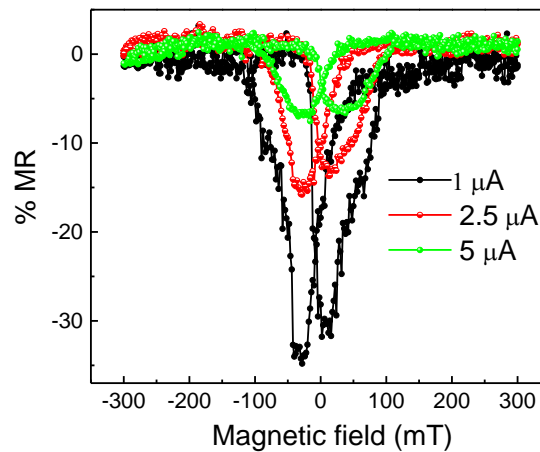


Fig. 5. Resistance of a LSMO/Alq₃/Co organic spin valve as a function of in-plane magnetic field obtained at 10 K and three different currents.

Our experimental data is in good agreement with previously published results on Alq₃-based spin-valves [8, 41, 42] and MTJs [43], confirming reproducible device fabrication and characterization. The absence of a GMR response in our CoPc-based spin valves is therefore not due to experimental artefacts. This result is intriguing because encouraging spin-selective

interface (“spinterface”) formation between phthalocyanine molecules and FM metals has been shown recently [23] and high GMR values have been measured on other phthalocyanine-based spin valves [38]. To clarify the possible physical origins behind the lack of GMR in CoPc-based spin valves, we performed detailed photoelectron spectroscopy, magnetic and magnetotransport measurements on our FM/OS interfaces. As an initial working hypothesis we investigate the two most probable reasons for the absence of GMR: (1) inefficient spin injection at the FM metal/CoPc interfaces and (2) strong spin relaxation in the CoPc layer. We first consider the properties of the FM/CoPc interfaces.

3.2. Electronic structure of FM/OS interface

In our previous study on LSMO/region-regular P3HT interfaces [9], we showed that the organic layer strongly binds to the LSMO electrode. It has also been shown by different groups that the binding is mainly due to a chemisorption process based on charge transfer between the metal/half-metal and the organic molecules, which results in the formation of a strong interface dipole [44]. The interface dipole effectively modifies the electronic properties of the FM/OS interface and this can affect spin injection in spin-valve devices. To study the electronic properties of the LSMO/CoPc interface, we performed x-ray photoelectron spectroscopy (XPS) measurements on different samples: A pristine LSMO film, LSMO covered with a 5 nm and 15 nm thick CoPc layer, and the same sample after washing the CoPc layer off. Because data on the Phthalocyanine/Co top interface has been published previously [45], we do not study this interface here. The XPS results show clear differences between the pristine LSMO core level spectra, pure CoPc spectra, and interface hybrid states. Figure 6 shows Mn $3s$, O $1s$ and C $1s$ spectra from the four samples without any specific surface treatments. It can be seen that the O $1s$ and C $1s$ peaks are modified by the application and subsequent removal of the CoPc layer.

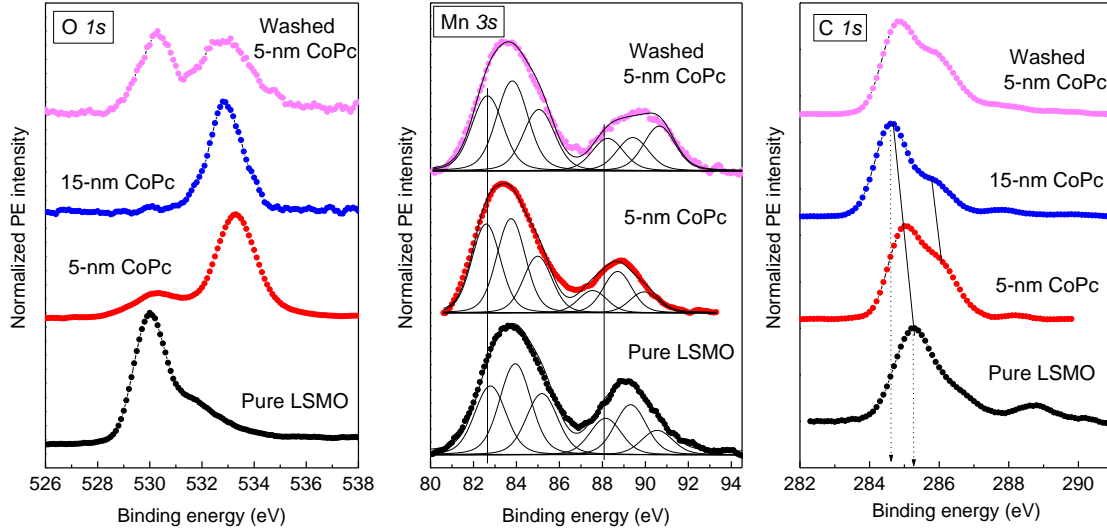


Fig. 6: O $1s$, Mn $3s$, and C $1s$ core level photo-emission spectra of pure LSMO films, LSMO coated with 5 nm and 15 nm of CoPc, and LSMO after washing the CoPc layer with acetone and alcohol.

For the pristine LSMO film, an O $1s$ peak around 530 eV is measured with a little shoulder on the higher binding energy side. This high energy shoulder is most probably caused by surface contamination (the surface was not specially treated or cleaned before XPS to keep the device-like conditions intact), which is consistent with the appearance of a C $1s$ signal. The surface contamination, which can diffuse towards the CoPc film, may be the result of physisorbed, chemisorbed, and structural H_2O together with hydroxide (OH^-) and CO_2 contributions [46]. Both CoPc-covered samples also contain oxygen due to their exposure to air. The main O $1s$ peak consists of three components arising from the three different oxide layers in the crystal lattice. In the case of LSMO, the binding energies of the three components from the higher to the lower binding energy side can be assigned to Mn–O, La–O, and Sr–O, respectively [47]. In the present case, we see that the application and subsequent removal of the CoPc layer slightly moves the LSMO O $1s$ peak towards higher binding energy, which suggests a change in Mn–O bonding environments. For CoPc, it has been previously reported that the O $1s$ peak originates from the adsorption of atomic O into the organic layer leading to the formation of a metal-oxygen ligand [48]. Compared to the 5 nm CoPc coated sample, the peak position of the 15 nm sample is slightly shifted towards lower binding energy and the peak broadens for the washed sample. This evolution indicates that additional bonding between O and N and C may take place.

For FePc molecules, it has been shown that atomic oxygen adsorption changes the lineshape and intensity ratio of the peaks in the C *1s* spectrum due to the emission from benzene (C=C) to pyrrole (C=N) carbon atoms [49]. However, in our case only some minor changes in the Co *2p* lineshape are observed in the 5 nm and 15 nm thick CoPc films on LSMO and the washed sample does not show any shift of the binding energy in the Co *2p* and N *1s* spectra (not shown here). For Mn *3s*, the exchange splitting of the Mn *3s* electronic state (i.e., the peaks around 83 and 89 eV) does not modify significantly after the application of a CoPc layer. For the sample with 15 nm CoPc coverage, the Mn peaks could not be clearly identified. Earlier, de Jong et al. [50] reported that the magnitude of the splitting of Mn *3s* peaks in LSMO is associated with the amount of *3d* electrons and therefore the average valence of the Mn ions. Fits of the Mn *3s* spectra show the presence of three components around binding energies of 83 eV and 89 eV. Here, we included a minimum number of components to obtain a good fit. Although it is well known that spectral line fitting is not unambiguous, the presence of six peaks is fully supported by details of the experimental line shapes (e.g. shoulders and asymmetries). The extracted shifts of the second and third peaks with respect to the first peak amount about +1.2 eV and +2.4 eV. The individual components are most likely reflecting three different bonding environments (or chemical sites) for Mn atoms in the surface region of the LSMO film.

In the C *1s* spectrum of the pristine LSMO film, the main peak is dominated by carbon contamination from the atmosphere. However, when covered by CoPc the spectrum becomes broad and an additional shoulder emerges at higher binding energy. From lower to higher binding energy, the peaks generally denote benzene and pyrrole bonding. Upon additional CoPc coverage (15 nm), the C *1s* peak moves towards lower energy, yet the lineshape remains almost constant. After removal of CoPc, the C *1s* spectra does not change substantially. Thus, the presence of Co *2p*, N *1s*, higher binding energy O *1s*, C *1s* and modified Mn *3s* peaks clearly signifies strong bonding of CoPc to the LSMO surface with a modification of the electronic interface states as result.

3.3. Magnetic and transport properties of FM/OS interfaces

Previously, it has been shown by x-ray magnetic circular dichroism (XMCD) that adsorption of 1 monolayer (ML) of Mn-phthalocyanine (MnPc) molecules decreases the magnetic moment of Co from 1.73 μ_B to 1.67 μ_B (supplementary information of Ref. 23). From on-site local

magnetization density maps, it was also concluded that a strong antiferromagnetic (AFM) coupling between Co and C benzene sites leads to a reduction of the total magnetic moment of Co by $0.22 \mu_B$ for all C atoms [23]. Although Iacovita et al. [51] have shown ferromagnetic interactions at the interface between CoPc molecules and Co nano-islands, they predicted that hybridization between Co $3d$ and N $2p$ states results in a reduced magnetic moment of $0.7 \mu_B$. Several other groups [52, 53] have also reported on a change in the Co $3d$ electronic distribution due to chemisorption and subsequently hybridization with phthalocyanine molecules leading to a suppressed magnetic moment of CoPc on Co or Fe substrates. The electronic modifications at the CoPc/FM interface not only change the magnetic properties, but likely affect spin injection at such interfaces. However, all these studies report on the magnetic properties of a FM metal when phthalocyanine molecules are deposited on top of the FM electrode. It is therefore interesting to obtain insights into the magnetic properties of Co when it is evaporated on top of phthalocyanine molecules (i.e. when Co is used as top electrode). To study this, we recorded magnetic hysteresis loop (M - B) for (a) a single CoPc (120 nm) layer, (b) a Co (8 nm)/Al (120 nm) bilayer, and (c) a CoPc (120 nm)/Co (8 nm)/Al (100 nm) trilayer using SQUID magnetometry at 10 K, 100 K, and 300 K. The M - B loops for the Co/Al bilayer and CoPc/Co/Al trilayer at 10 K are shown in Figure 7.

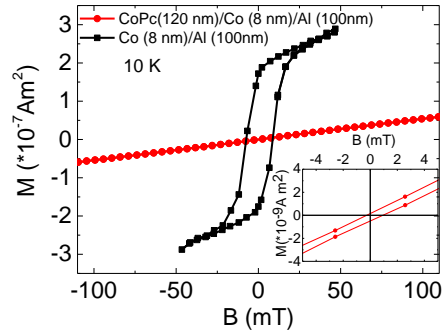


Fig. 7. Magnetic hysteresis loops of a Co (8 nm)/Al (120 nm) bilayer (squares) and a CoPc (120nm)/Co (8nm)/Al (100 nm) trilayer (circles) recorded at 10 K.

The results suggest that 120 nm thick CoPc is purely paramagnetic (not shown here). The 8 nm thick Co film is ferromagnetic with a coercive field of 5 mT. The Co magnetic moment is drastically suppressed when it is evaporated on top of CoPc molecules. This result can be explained by systematic analysis of data reported in literature. For instance, photoemission

spectroscopy data from Schmitt et al. [45] show Co diffusion into the metal-Pc layer and the formation of nano-sized Co clusters rather than a continuous Co film when Co is used as top electrode. The study also shows that chemical reactions at the interface occur mainly by the oxidation of the Co layer. This oxidation process can be attributed either to the presence of residual gas in the deposition chamber or a reaction with the central metal atom of phthalocyanines. Recent results show that the magnetic state of cobalt oxide nanoparticles can be complex and effects such as coexisting weak ferromagnetism, exchange bias, etc. have been observed due to uncompensated spin on the surface and core of nanoparticles and exchange coupling between FM and AFM layers [54]. In any case, compared to pure Co, the magnetization of oxidized Co is much weaker (pure cobalt oxide is antiferromagnetic). Also, it has been shown that hydrogen atoms of the organic molecule form a strong H-Co bond via a chemical reaction, which reduces the surface magnetization of the Co film [55]. The interaction between the π -electrons of the organic molecule and the $3d$ electrons of the FM metal is anticipated to change the electronic states at the interface leading to modified interface magnetization. For example, density functional theory studies predict that the spin polarization at the interface changes as a function of the distance between the benzene ring and the FM metal [56]. Based on these observations and our experimental results, we conclude that the magnetization and spin polarization of the CoPc/Co interface are not very good causing inefficient spin injection and detection.

To check the spin injection properties of the LSMO/CoPc bottom interface, we performed magnetic measurements on LSMO films coated with 5 nm, 10 nm, and 15 nm thick CoPc layers and the results are compared with the magnetic properties of pristine LSMO films (Figure 8). The M - T data show that the saturation magnetization (M_S) and Curie temperature (T_C) of the LSMO film are increased when the film is covered by CoPc. For the 5 nm coating, the saturation magnetization increases by almost 20% and T_C increases by about 30 K (~10%). For the 10 nm and 15 nm CoPc coatings, the M_S value decreases slightly, however, T_C still enhances for the 10 nm coating. No further changes in T_C are observed for the 15 nm CoPc coating. The results indicate that chemisorption of CoPc on LSMO enhances the magnetic properties of LSMO. Also, the M - B loops show more abrupt switching and a decrease of the coercive field (H_C) by nearly 18% after deposition of CoPc on LSMO. The LSMO/CoPc interactions do not only affect the interface layers of the metal oxide and OS, but also change the electronic configuration of

subsequent layers up to a CoPc thickness of 10 nm. In LSMO, ferromagnetism arises from double-exchange interactions between mixed valence states of the Mn^{3+} and Mn^{4+} ions and hopping of e_g electrons via oxygen ligands [39]. The hopping of e_g electrons are critically dependent on the Mn-O bond length and Mn-O-Mn bond angle. Also, the ratio between Mn^{3+} and Mn^{4+} ions controls the ferromagnetic interactions and because oxygen atoms change Mn^{3+} into Mn^{4+} , they modify the FM properties significantly. Therefore, the amount and position of oxygen atoms in the LSMO lattice plays a major role in determining ferromagnetism in LSMO. Also, it is well known that the abrupt discontinuation of oxygen bonds at the LSMO surface degrades the magnetic properties of the surface layers [57]. Our XPS data indicate the presence of additional oxygen peaks when the films are covered by 5 nm and 15 nm of CoPc and the oxygen peaks remain after washing the films with acetone and alcohol. This suggests that the oxygen layer of CoPc is chemically bonded to the LSMO. As a result, the amount of dangling oxygen bonds at the LSMO surface is reduced and the magnetic properties of LSMO surface are enhanced. Our data are in line with a SHIPS model [45], which also predicts an increase of the effective spin polarization of electrodes due to Ba with OS molecules such as Alq_3 .

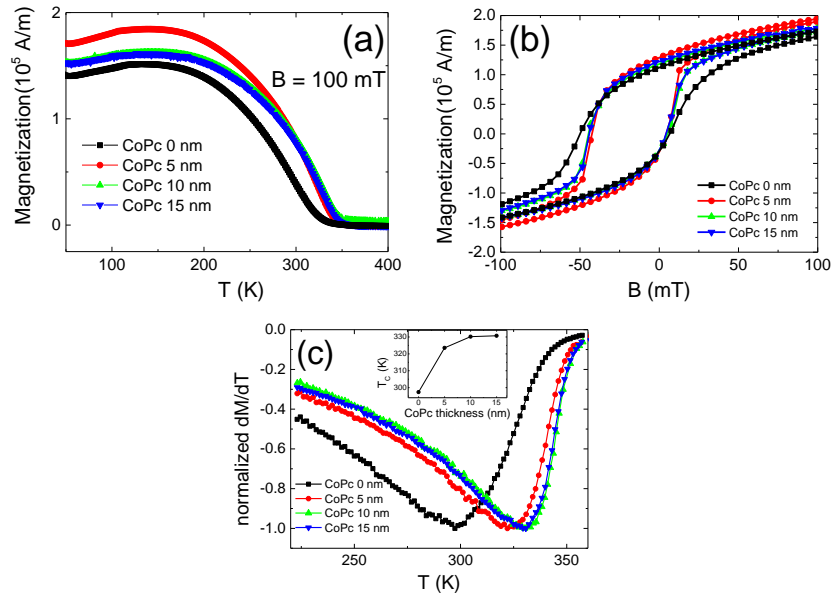


Fig. 8. Magnetization (M) as a function of (a) temperature (T) and (b) magnetic field (B) for pristine LSMO films and LSMO films coated with 5 nm, 10 nm, and 15 nm of CoPc. (c) First derivative (normalized) of M as a function of T . The inset shows the extracted Curie temperature as a function of CoPc film thickness.

In addition to the magnetic properties, it is also important to understand the magnetotransport properties of the LSMO/CoPc interface. Here, we present magnetotransport measurements of pristine and CoPc-coated LSMO films, which were conducted by varying the magnetic field between -300 mT and +300 mT at 10 K. The data show that the adsorption of CoPc substantially increases the negative magnetoresistance of the LSMO films. This result is intriguing considering the fact that due to improved oxygen bonding, the magnetic properties of the LSMO/CoPc interface are enhanced and better metallic conduction is anticipated. However, previously it has been shown that the application of region-regular poly(3-hexyl thiophene) on LSMO increases the LSMO sheet resistance due to the formation of interfacial defects, dipole formation, and chemical reactions [58]. Also, XPS shows that traces of Co, N and C atoms are present at the LSMO interface even after the CoPc layer is washed off. Based on this, we conclude that CoPc deposition on LSMO enhances the defect sites at the LSMO/CoPc interface, which results in an increased scattering and trapping of charge carriers. The application of magnetic field suppresses the scattering leading to larger negative magnetoresistance in the LSMO/CoPc bilayer compared to the pristine LSMO film. Previously, charge trapping domains at the LSMO/Alq₃ interface have also been reported by Prezioso et al. [59]. However, the nature of such defect sites at the LSMO/CoPc interface is not very clear and requires further investigation.

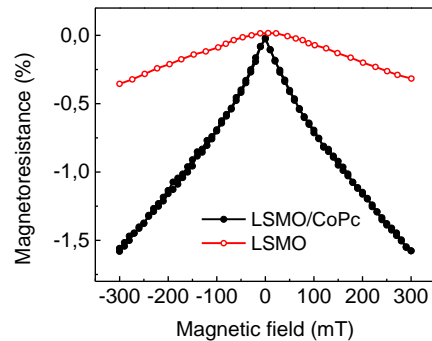


Fig. 9. Magnetoresistance of a LSMO film and a LSMO film coated by CoPc as a function of in-plane magnetic field at 10 K.

3.4. Spin transport properties of Co-Phthalocyanine layer

Our experiments show that Co diffusion and the formation of nano-islands at the top interface of organic spin valves degrade the magnetic properties and pose limitations on the efficiency of spin injection and detection at this interface. Also, the injection barrier height is modified by chemical reactions between Co and the CoPc molecule. For the LSMO electrode, the magnetic and spin polarization properties of the LSMO/CoPc interface are improved, but the observation of a significant low-field magnetoresistance effect suggests the formation of scattering and trapping sites at this interface. Hence, we infer that relatively good spin injection at this interface is likely, but low conductivity domains cannot be avoided. In addition, enhanced spin relaxation inside the CoPc spacer layer cannot be ruled out due to the presence of Co, which has a larger atomic weight than Al in Alq₃. Spin-valves with a ~100 nm thick CuPc spacer and Co and Fe electrodes, for example, have been found to exhibit a similar GMR response as Alq₃ based spin valves [60]. On the other hand, Yue et al., [61] have shown that the GMR of hybrid CuPc/Alq₃ junctions with a LSMO bottom and a Co top electrode is substantially decreased (by almost one order of magnitude) compared to single-barrier LSMO/Alq₃/Co junctions. This large decrease of GMR was attributed to the inferior spin injection properties of the LSMO/CuPc interface due to a lowering of the injection barrier. The injection barrier heights of CoPc and CuPc electrodes are very similar [62]. Therefore, at least some spin injection should occur in our CoPc-based spin valves. The complete absence of GMR suggests that an injection barrier effect cannot fully explain the magnetotransport properties of the LSMO/CoPc/Co devices.

A direct comparison of the spin transport properties of Alq₃ and CoPc layers is complicated by a lack of data on spin diffusion lengths and spin relaxation times from identical experiments. Spin relaxation time measurements on CoPc molecules based on optical techniques and magnetotransport data of Alq₃ molecules, however, provide some information. Gadalla et al. [63] reported on ultrafast spin relaxation dynamics in CoPc molecules and metal free H₂Pc molecules. Their study shows that the spin relaxation time in CoPc is of the order of a few picoseconds (10^{-12} s), which is similar to other phthalocyanin molecules containing transition metal ions [64]. The fast spin relaxation in CoPc was attributed to the presence of Co atoms. Coupling between π -orbital of molecules and the d -electrons of the transition metals is capable of providing additional channels for energy relaxation or fast relaxation via a charge transfer process. Therefore, it seems viable that although the LSMO/CoPc interface is suitable for spin injection, the spin polarization fully relaxes inside the CoPc spacer before the carriers traverse the 120 nm wide channel. In Alq₃

molecules, on the other hand, the spin relaxation time is of the order of a few milliseconds [65], which allow charge carriers to retain their spin state over a large distance (up to hundreds of nanometers) at low temperature.

The spin diffusion length is defined as $\lambda_S = \sqrt{D_S T_S}$, where D_S is the diffusion coefficient and T_S is the spin relaxation time. D_S is proportional to the mobility of the material ($D = \mu k_B T$) and it is almost of the same order of magnitude for amorphous Alq₃ [66] and CoPc molecules [67] with CoPc having slightly higher mobility. An approximately six orders of magnitude difference in T_S (although comparison of real numerical value is unrealistic) would therefore lead to a three orders of magnitude difference in spin diffusion length between CoPc and Alq₃. For most OS molecules the spin relaxation time is of the order of 10^{-3} to 10^{-6} s and, hence, large spin relaxation lengths can be expected. For metal-organic molecules, however, the zero field splitting value is rather large ($\sim 200 \text{ cm}^{-1}$) compared to compounds without metal atoms ($\sim 0.1 \text{ cm}^{-1}$), which indicates substantially stronger spin-orbit coupling in these compounds [68]. The fast spin relaxation in organic materials with heavy metals makes them an unattractive choice for spin transport devices.

In addition, organic compounds containing heavy metals are capable of producing charge scattering and trapping sites at the electrode/spacer interface and this can also contribute to the absence of GMR in spin-valves. Future spin transport measurements on a variety of transition metal-phthalocyanin molecules as a function of spacer thickness could provide more information on these issues.

Conclusions

We have studied the spin injection and transport properties of organic spin valves with two different organic spacers, namely Alq₃ and CoPc, sandwiched between half-metallic LSMO and Co electrodes. While Alq₃-based spin valves demonstrate clear and reproducible magnetic switching with almost 35% negative GMR, the CoPc-based spin valves do not show any GMR response. Magnetic and magnetotransport measurements of the FM/CoPc interface indicate that the ferromagnetic properties of the LSMO interface are improved by a reduction of dangling oxygen bonds, but detrimental charge trapping sites are formed due to adsorption of Co, N, and

C atoms. Diffusion of Co into the OS layer and chemical reactions between Co and the OS degrade the magnetic properties and spin injection properties of the Co top electrode. Finally, fast spin relaxation inside the CoPc spacer layer due to the presence of heavy Co atoms and associated strong spin-orbit coupling makes CoPc unsuitable for organic spin-valve devices. In summary, the absence of GMR in CoPc-based spin valves is explained by a combined effect of inefficient spin injection and poor spin transport.

Acknowledgement

The authors gratefully acknowledge financial support from Jenny and Antti Wihuri Foundation, Centre for International Mobility (CIMO) grant, Turku Collegium for Science and Medicine (TCSM) and COST Action MP1202 (HINT).

Reference

- [1] S. D. Bader and S. S. P. Parkin, *Ann. Rev. Condens. Mat. Phys.* **1**, 71 (2010).
- [2] S. A. Wolf et al., *Science* **294**, 1488 (2001).
- [3] W. J. M. Naber et al., *J. Phys. D: Appl. Phys.* **40**, R205 (2007).
- [4] S. Majumdar, H.S. Majumdar, R. Österbacka, *Comprehensive Nanoscience and Technology*, vol. **1**, (Oxford Academic Press, 2011) pp. 109–142.
- [5] V. Dediu, L. E. Hueso, I. Bergenti, C. Taliani, *Nat. Mater.* **8**, 707 (2009).
- [6] D. Sun et al., *Chem. Commun.* **50**, 1781 (2014).
- [7] V. Dediu et al., *Solid State Commun.* **122**, 181 (2002).
- [8] Z. H. Xiong, D. Wu, Z. V. Vardeny, J. Shi, *Nature* **427**, 821 (2004).
- [9] S. Majumdar et al., *Appl. Phys. Lett.* **89**, 122114 (2006).
- [10] J. –W. Yoo et al., *Synth. Met.* **160**, 216 (2010).
- [11] D. Sun et al., *Phys. Rev. Lett.* **104**, 236602 (2010).
- [12] X. Zhang et al., *Nature Commun.* **4**, 1392 (2013).
- [13] T. S. Santos et al., *Phys. Rev. Lett.* **98**, 016601 (2007).
- [14] J. J. Schoonus et al, *Phys. Rev. Lett.* **103**, 146601 (2009).
- [15] J. S. Jiang, J. E. Pearson, S. D. Bader, *Phys. Rev. B* **77**, 035303(2008).
- [16] A. Riminucci et al., *Appl. Phys. Lett.* **102**, 092407 (2013).
- [17] F. J. Wang, C. G. Yang and Z. Valy Vardeny, *Phys. Rev. B* **75**, 2453241 (2007).
- [18] A. J. Drew et al., *Nature Mater.* **8**, 109 (2009).
- [19] S. Majumdar and H. S. Majumdar, *Org. Electron* **13**, 2653 (2012).
- [20] S. Majumdar and H. S. Majumdar, *Synth. Met.* **173**, 26 (2013).
- [21] S. Sanvito, *Nature Phys.* **6**, 562 (2010).
- [22] M. Cinchetti et al., *Nature Mater.* **8**, 115 (2009).
- [23] F. Djeghloul et al., *Sci. Rep.* **3**, 1272 (2013).
- [24] Y. Zhan and M. Fahlman, *J. Polym. Sci. B* **50**, 1453 (2012).
- [25] N. Atodiressei, et al., *Phys. Rev. Lett.* **105**, 066601 (2010).
- [26] T. L. Francis et al., *New J. Phys.* **6**, 185 (2004).
- [27] S.-T. Pham, Y. Kawasugi and H. Tada, *Appl. Phys. Lett.* **103**, 143301 (2013).
- [28] P. A. Bobbert et al., *Phys. Rev. Lett.* **102**, 156604 (2009).
- [29] S. Majumdar et al., *Phys. Rev. B* **79**, 201202(R) (2009).

- [30] F. Wang and Z. V. Vardeny, *Synth. Met.* **160**, 210 (2010).
- [31] S. Majumdar, H. S. Majumdar, H. Aarnio, and R. Österbacka, *Phys. Stat. Solidi RRL* **3**, 242 (2009).
- [32] W. Wagemans, P. Janssen, E.H.M. van der Heijden, et al., *Appl. Phys. Lett.* **97**, 123301 (2010).
- [33] H. Laurs and G. Heiland, *Thin Solid Films* **149**, 129 (1987).
- [34] G. de la Torre et al., *Chem. Rev.* **104**, 3723 (2004).
- [35] S. Ambily and C. S. Menon, *Thin Solid Films* **347**, 284 (1999).
- [36] P. E. Fielding and F. Gutman, *J. Chem. Phys.* **26**, 411 (1957).
- [37] E. Annese et al., *Phys. Rev. B* **84**, 174443 (2011).
- [38] S. Schmaus et al., *Nature Nanotech.* **6**, 185 (2011).
- [39] S. Majumdar and S. van Dijken, *J. Phys. D: Appl. Phys.* **47**, 034010 (2014).
- [40] S. Majumdar et al., *J. Appl. Phys.* **104**, 033910 (2008).
- [41] B. Li et al., *Org. Electron.* **13**, 1261 (2012).
- [42] S. W. Jiang et al., *New J. Phys.* **16**, 013028 (2014).
- [43] C. Barraud et al., *Nature Phys.* **6**, 615 (2010).
- [44] Y. Zhan et al., *Phys. Rev. B* **76**, 045406 (2007).
- [45] F. Schmitt et al., *Anal Bioanal Chem* **400**, 665 (2011).
- [46] S. Yamamoto, et al., *J. Phys. Chem. C* **111**, 7848 (2007).
- [47] S. Majumdar et al., *J. Phys.: Condens. Mat.* **25**, 376003 (2013).
- [48] M. Tsuda, E. S. Dy and H. Kasai, *J. Chem. Phys.* **122**, 244719 (2005).
- [49] O. Snezhkova et al.,
<https://www.maxlab.lu.se/cmris/display?id=workspace://SpacesStore/4c5ad129-aada-48e0-b50d-a818ea381bae>
- [50] M. P. de Jong et al., *J. Appl. Phys.* **94**, 7292 (2003).
- [51] C. Iacovita et al. *Phys. Rev. Lett.* **101**, 116602 (2008).
- [52] X. Chen and M. Alouani, *Phys. Rev. B* **82**, 094443 (2010).
- [53] J. Brede et al., *Phys. Rev. Lett.* **105**, 047204 (2010).
- [54] F. Moro et al., *J. Magn. Mag. Mater.* **348**, 1 (2013).
- [55] S. Gallego et al., *Phys. Rev. B* **82**, 085414 (2010).
- [56] S. G. Said et al., *J. Appl. Phys.* **113**, 013905 (2013).

- [57] V. Garcia et al., Phys. Rev. B **69**, 052403 (2004).
- [58] M. Pesonen et al., AIP Advances **3**, 042102 (2013).
- [59] M. Prezioso et al., Adv. Mater. **23**, 1371 (2011).
- [60] Y. Liu et al., J. Appl. Phys. **105**, 07C708 (2009).
- [61] F. J. Yue et al., Appl. Phys. Lett. **101**, 022416 (2012).
- [62] P. -C. Kao et al., J. Electrochem. Soc., **153** (6) H122 (2006).
- [63] A. Gadalla et al., J. Phys. Chem. C **114**, 17854 (2010).
- [64] A. V. Nikolaitchik et al., J. Phys. Chem. A **103**, 7597 (1999).
- [65] S. Pramanik et al., Nature Nanotech. **2**, 216 (2007).
- [66] G. G. Malliaras et al., Appl. Phys. Lett. **79**, 2582 (2001).
- [67] M. Bora, D. Schut and M. A. Baldo, Anal. Chem. **79**, 3298 (2007).
- [68] H. Yersin and J. Strasser, Coord. Chem. Rev. **208**, 331 (2000).